Journal of Applied Polymer Science

Synergistic Effects by Compatibilization and Annealing Treatment of Metallocene Polyethylene/PLA Blends

Sun-Mou Lai,[1] Kun-Che Hung,[1] Hui Cheng Kao,[2] Liang-Chuan Liu,[2] Xue Fen Wang[1]

[1]Department of Chemical and Materials Engineering, National I-Lan University, I-Lan 260, Taiwan, ROC

[2]Yomura Technologies, Inc., New Taipei City, Taiwan, ROC

Correspondence to: S.-M. Lai (E-mail: smlai@niu.edu.tw)

ABSTRACT: The properties of metallocene polyethylene (mPE)/polylactic acid (PLA) bio-based blends containing an ethylene-glycidyl methacrylate-vinyl acetate (EGMA-VA) compatibilizer, with or without the annealing effect of PLA were investigated. The results from SEM (Scanning electron microscope) morphology observation revealed that the dispersed PLA particles sizes within the mPE matrix tended to decrease with the added compatibilizer due to the enhanced interfacial interaction. DSC (Differential scanning calorimetry) and XRD (X-ray diffractometer) results indicated that the addition of the compatibilizer completely hindered the cold crystallization and rearrangement crystallization of PLA, even though the additional annealing effect tended to increase the crystallization of PLA. Tensile test results showed the synergistic effects by compatibilization and annealing treatment improved the tensile strength and Young's modulus, up to 38 % and 62 % increase, respectively. With the incorporation of the compatibilizer, the viscosity increased and reached the highest level among all neat resins and blends, which was attributed to the enhanced interfacial interaction between mPE and PLA. Hopefully, the incorporated bio-based PLA materials could be helpful in reducing the use of petroleum-based materials and are beneficial to the environment in terms of the sustainable development concern. © 2013 Wiley Periodicals, Inc. J. Appl. Polym. Sci. 130: 2399–2409, 2013

KEYWORDS: Metallocene polyethylene, polylactic acid (PLA), compatibilizer, annealing

Received 26 November 2012; accepted 19 April 2013; Published online 25 May 2013

DOI: 10.1002/app.39437

INTRODUCTION

A polymer blending technique without solvent hazard to prepare novel materials receives much attention in the scientific and industrial community due to its cost-competitive merit. Biodegradable polymers featuring ecological advantages toward sustainable development have been of great commercial interest due to a growing environmental concern.[1] In particular, polylactic acid (PLA), synthesized through the lactide from the fermentation of the sugar feedstock, such as corn, etc., has been considered as a fascinating bio-based polymer in light of its biocompatibility, non-toxicity, and biodegradability.[2] Owing to the aforementioned characteristics, the material could be used in numerous biomedical and environmental applications, including suture, bone screw, plastic film, etc. As the production of PLA did not rely on petroleum resources, the field of application should not be solely focused on the biodegradability. Polymer blends containing PLA would exploit this renewable concept to reduce the environmental impact by cutting down the use of petroleum-based polymers.

Polyethylene-based polymers have been widely used in the industry. Blending of polyethylene and PLA could expand their applications by taking advantage of each characteristic. However, only a few works investigated the PLA/polyethylene blends until recently.[3–6] Anderson et al.[4] contrasted amorphous PLA and semicrystalline PLA on their blends with linear low density polyethylene (LLDPE). It was found that semicrystalline PLA showed significantly better adhesion to LLDPE than amorphous PLA, attributed to tacticty effects on the entanglement molecular weight or miscibility of polylactic acid. Our recent work[5] reported that a commercialized ethylene–glycidyl methacrylate copolymer (EGMA) was applied as a compatibilizer to improve the dispersion and interaction of dispersed metallocene polyethylene within the PLA matrix. Su et al.[6] studied the compatibility of PLA/glycidyl methacrylate grafted poly(ethylene octene) (GMA-*g*-POE) blends. Enhanced compatibility was reached by the interfacial reactions between the carboxyl groups of PLA and epoxy groups of GMA-*g*-POE. These compatibilizing techniques are quite useful to improve the performance of PLA/PE blends

In order to exploit this renewable natural resource to form bioplastic blends, nonpolar metallocene polyethylene elastomer (mPE) was selected as a matrix to blend with PLA serving as a

minor component. This design is in contrary to most systems in the literature which generally selected PLA as a matrix. By incorporating bio-based PLA within the petroleum-based matrix, it would be beneficial to the environmental sustainability due to the reduced usage of petroleum-based materials. Potential applications include smart phone cover, foam products, etc. Similarly, an ethylene–glycidyl methacrylate–vinyl acetate copolymer was added to improve the interfacial strength of mPE/PLA blends. In addition, it was reported that the annealing effect of PLA could enhance the re-crystallization phenomenon.[7] In this study, we will use semicrystalline PLA, instead of amorphous PLA in our previous study,[5] to investigate the annealing effect on the compatibilized systems. This study attempts to elucidate both compatibilization and annealing effects together in terms of domain dispersion, thermal properties, tensile properties, and rheological properties. To the best of authors' knowledge, this study is the first attempt to discuss the synergistic strengthening effects by compatibilized interphase and annealed dispersed phase of PLA. Hopefully, this will pave the way for the innovative development of bio-based polymers in targeted applications, including automotive and sport components, etc. in terms of environmental concern.

EXPERIMENTAL

Materials

MPE with a melt flow index of 1 g/10 min and a density of 0.885 g/cm^3 with the trade name Engage 8003 was supplied by Dow Corporation, corresponding to octene comonomer contents (%) of 30. PLA was supplied from NatureWorks LLC under the trade name of 4032D corresponding to L-isomer contents (%) of 98.7. Ethylene–glycidyl methacrylate–vinyl acetate copolymer (EGMA–VA, Sumitomo Chemical Company, IGETABOND® 2B) with a melt flow index of 3 g/10 min was used as a neat compatibilizer. Grafting levels of glycidyl methacrylate and vinyl acetate are reported to be 12 and 5 wt %, respectively.

Sample Preparations

PLA was pre-dried for 4 h at 80°C. MPE and EGMA–VA were pre-dried for 6 h at 50°C. The blend composition of mPE and PLA was fixed at a weight ratio of 80/20. The compatibilizer was loaded at a composition of 10 phr (parts per hundred resins of mPE and PLA blend). Mixing was carried out under 50 rpm at 180°C for 10 min using a batch mixer (Brabender 815605, Plastograph). All blends were predried for 4 h at 65°C in a vacuum oven. The prepared samples were then hot-pressed at 180°C to obtain sheets about 1 mm thick. For materials subjected to annealing treatment, the annealing condition was set at 125°C for 2.5 h in the hot press.

Measurements

Structure Characterization. The Fourier transform infrared spectra (FTIR) to assess the reaction between EGMA–VA and PLA were recorded using a spectrophotometer (Spectrum 100, Perkin-Elmer) at a resolution of 4 cm^{-1} for 32 scans from 650 to 4000 cm^{-1}. X-ray diffraction (XRD) techniques were employed to evaluate the crystalline structure of the samples.[8,9] No "]" A Rigaku-Ultima IV X-ray unit, operating at 40 kV and 20 mA, was used for the experiments at room temperature. The X-ray source was Cu $K\alpha$ radiation. The diffractograms were scanned in the 2θ range from 10° to 50° at a rate of 1.8°/min.

Morphological Characterization. The morphology of the cryo-fractured surface of specimens followed by extraction with chloroform at room temperature for 2.5 h to remove PLA domains was elucidated with the scanning electron microscope (SEM; TESCAN, 5136 MM).[10] All samples were sputtered with gold before microscopic observations. The mean cavity sizes of etched PLA domains were measured using an IMAGE J software. Thirty cavities per image were averaged to calculate the mean cavity sizes.

Thermal Characterization. The crystallization temperature (T_c), glass transition temperature (T_g), and melting temperature (T_m) were determined using a differential scanning calorimetry (DSC; DSC Q10, TA). The sample was cooled to −70°C before first run, and then heated to 200°C at a heating rate of 10 °C/min. Then, the sample was cooled down to −70°C at 10°C/min and heated to 200°C again at 10°C/min to complete the second run. The crystallinity of mPE was determined by taking the heat of fusion divided by the actual mPE content and the enthalpy required for 100% crystallinity, equal to 289 J/g.[11] The crystallinity of PLA was calculated by the similar approach using the enthalpy required for 100% crystallinity of PLA, equal to 135 J/g.[12] Dynamic mechanical thermal properties of blends such as storage modulus (E'), loss modulus (E''), and damping peak (tan δ) were measured using a dynamical mechanical thermal analyzer (Pyris Diamond, Perkin Elmer). The measurements were carried out in the tension mode at the frequency of 1 Hz from −80 to 75°C at a heating rate of 5°C/min.

Tensile Testing. Tensile measurements were conducted based on ASTM-D638 at a crosshead speed of 200 mm/min using an Instron 4469. Tensile strength, elongation at break, and Young's modulus were recorded.

Impact Testing. The notched Izod impact test complying with ASTM-D256 was performed using an impact tester (Gotech, GT-7045-C) at room temperature.

Rheological Analysis. Rheological measurements were carried out using a TA AR 2000 to determine the shear viscosity against shear rate from 0.1 to 100 (1/s) at 190°C.

RESULTS AND DISCUSSION

Structure Characterization. FTIR spectra of mPE/PLA blends are depicted in Figure 1 for comparison, including the neat resins and compatibilizer. The typical spectra of PLA included various functional groups such as C=O at 1750 cm^{-1}, C–O–C (Asymmetric) at 1134 cm^{-1}, C–O–C (Symmetric) at 1191 and 1092 cm^{-1}, and –CH$_3$ at 1456 and 1380 cm^{-1} in the 800–1800 cm^{-1} range were illustrated.[13,14] The characteristic absorption peak regions of epoxy (849, 912, and 995 cm^{-1}) and C=O (1735 cm^{-1}) for EGMA–VA were depicted as indicated in the literature.[6,15] As the compatibilizer was incorporated, most of typical absorption bands remained unchanged. No appearance of new absorption band was observed. In general, it was not clearly discernible on the compatibilized blends. In order to confirm the reaction of carboxyl group on PLA and epoxy group on the compatibilizer, PLA/EGMA–VA (50/50) blends

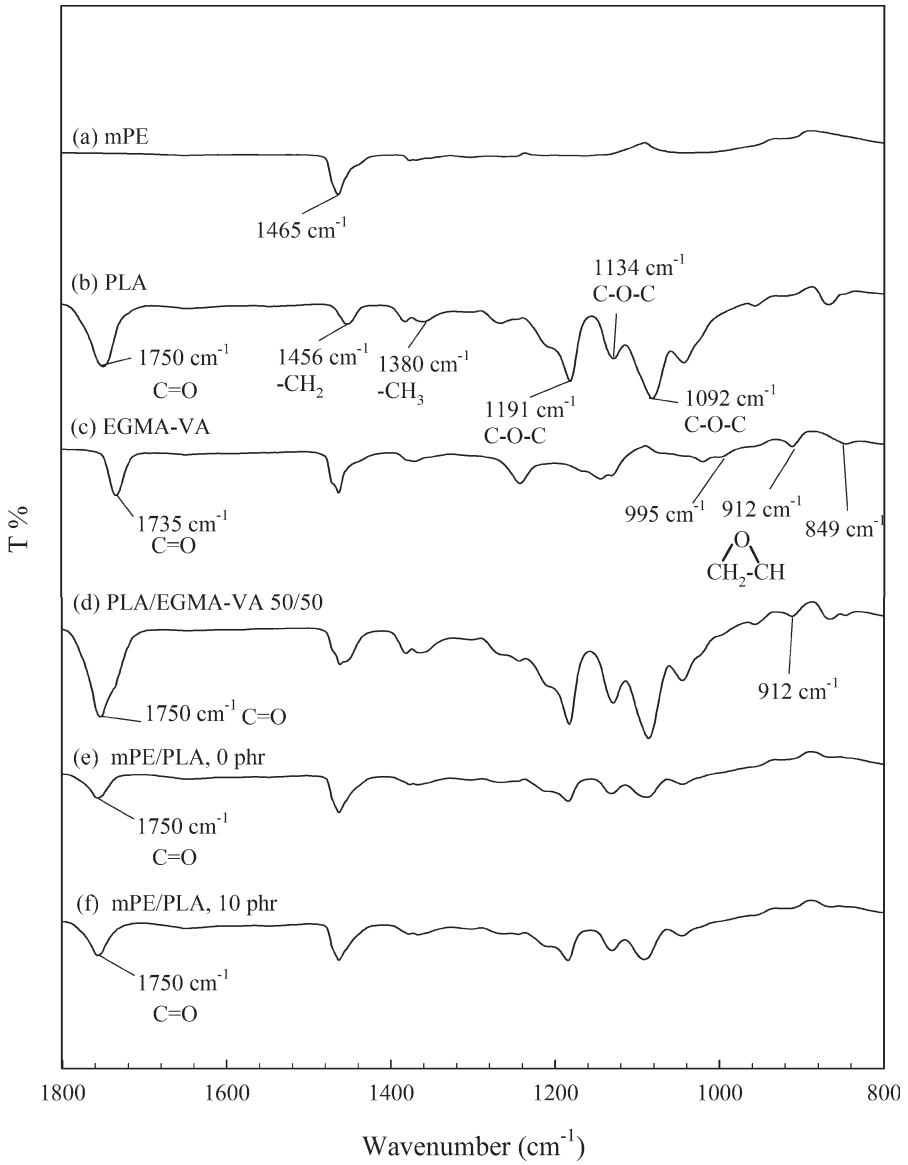

Figure 1. FT-IR spectra of mPE, EGMA-VA, PLA and mPE/PLA/EGMA-VA blends.

were prepared for justification. The epoxy peaks at 849 and 995 cm^{-1} disappeared and the carbonyl bands at 1735 cm^{-1} were slightly shifted after blending. This could be attributed to the aforementioned reaction between the epoxy groups on EGMA–VA and terminal carboxylic acid and/or the terminal hydroxyl groups on PLA involved in the blends.[6] In addition, the possible carbonyl group interactions between EGMA–VA and PLA were also suggested to contribute the carbonyl shift in the literature.[6]

Figure 2(a) shows the XRD patterns of neat PLA and PLA annealed at 125°C for 2.5 h. Neat PLA without the annealing treatment did not show clear diffraction patterns. On the other hand, diffraction peaks around 2θ at 14.0°, 16.6°, 19.0°, and 22.2° were observed for α form crystal planes at (010), (110), (203), and (105) for annealed PLA, respectively,[16] which indicated the crystallization behavior attained in the annealing process. For mPE/PLA blends, Figure 2(b) shows the XRD patterns of neat mPE, mPE/PLA blends with or without the compatibilization and annealing treatment. The characteristic diffraction peaks of 21.4° and 23.7° were corresponding to the mPE orthorhombic crystal planes (110) and (200), respectively, in combination with a broad amorphous halo.[17] The characteristic diffraction peaks of mPE in the mPE/PLA blends with and without EGMA–VA compatibilizer did not very much, except for the observed lower intensity. After annealing treatment, diffraction peaks of annealed PLA at 14.0° (010), 16.6° (110), and 19.0° (203) were observed. Note that for mPE/PLA blends upon annealing treatment, the relative characteristic peak intensity at 16.6° (110) of PLA to 21.4° (110) of mPE decreased with the addition of compatibilizer. In addition, characteristic crystal planes at (010) and (203) for PLA tended to disappear. This resulted from the diminished crystallization behaviors through

the limited mobility of PLA chains being reacted with EGMA–VA. The current result was in close agreement with the later discussion on the DSC analysis.

Dispersion Assessment

Figure 3 shows the distinct morphology of cryogenic fracture specimens for unmodified and compatibilized mPE/PLA blends before annealing at a specific composition of 80/20 based on the SEM observations. Dispersed particles with a dimension of a few μm in size represented PLA domains as shown in Figure 3(a) for mPE/PLA blends without compatibilizer. Figure 3(b) shows the morphology of mPE/PLA blends without compatibilizer subjected to chloroform extraction to remove PLA particles. Dispersed cavities with a dimension of about 1.88 $\pm$ 0.76 μm in size represented PLA domains. These observations clearly indicated a lack of specific interaction between PLA and mPE. Further, with addition of EGMA–VA, the mean particle sizes of PLA substantially decreased at 10 phr of compatibilizer as shown in Figure 3(c), suggesting a good interfacial bonding between mPE matrix and PLA dispersed phase. A substantial decrease in the cavity sizes (0.30 $\pm$ 0.13 μm) observed for the extracted morphology stemming from the enhanced interfacial interaction was elucidated as seen in Figure 3(d).

Figure 4 shows the results for the corresponding mPE/PLA blends after annealing treatment. The mean cavity sizes observed for the extracted morphology for mPE/PLA blends without compatibilizer and with compatibilizer were about 1.06 $\pm$ 0.51 and 0.68 $\pm$ 0.22 μm, respectively, indicating the enhanced interfacial interaction between mPE and PLA by compatibilization still remained even after annealing treatment. A small variation on the cavity sizes before and after annealing was observed, which might be due to the recrystallization and relaxation of molecular chains after annealing. A future study might be needed to investigate this interesting behavior.

Thermal Characterization

To have a better understanding on the thermal behaviors of blends, neat resins were conducted for comparison, as shown in Figure 5 and Table I. For brevity, only the thermal behaviors of cooling and second heating conditions were listed in Table I. The first heating process was only to eliminate thermal history, but one does find the recrystallization behavior of PLA, as seen in Figure 5(a). Thus, the crystallinity of PLA increased from 10.4% (before annealing) to 37.6% (after annealing) in a similar order what was reported in the literature,[18] although samples were not under controlled cooling process. As for mPE, the crystallinity was about 12.6% and the value was not varied much in the blends within experimental error in consideration of broad melting curves in all cases (curves in Figures 5 and 6). Thus, for brevity, those values were omitted without further comparison. The crystallization peak temperature value (T_c, temperature at the exotherm maximum) of mPE and EGMA–VA for the consecutive cooling process in Figure 5(b) was found to be about 61.8 and 80.0 °C, respectively. The determined T_g for PLA was estimated to be 55.2°C. For the second heating traces, Figure 5(c), the clear exothermic peak at 108.1°C depicted the cold crystallization behaviors for PLA. The crystallinity of PLA before and after annealing in the second heating

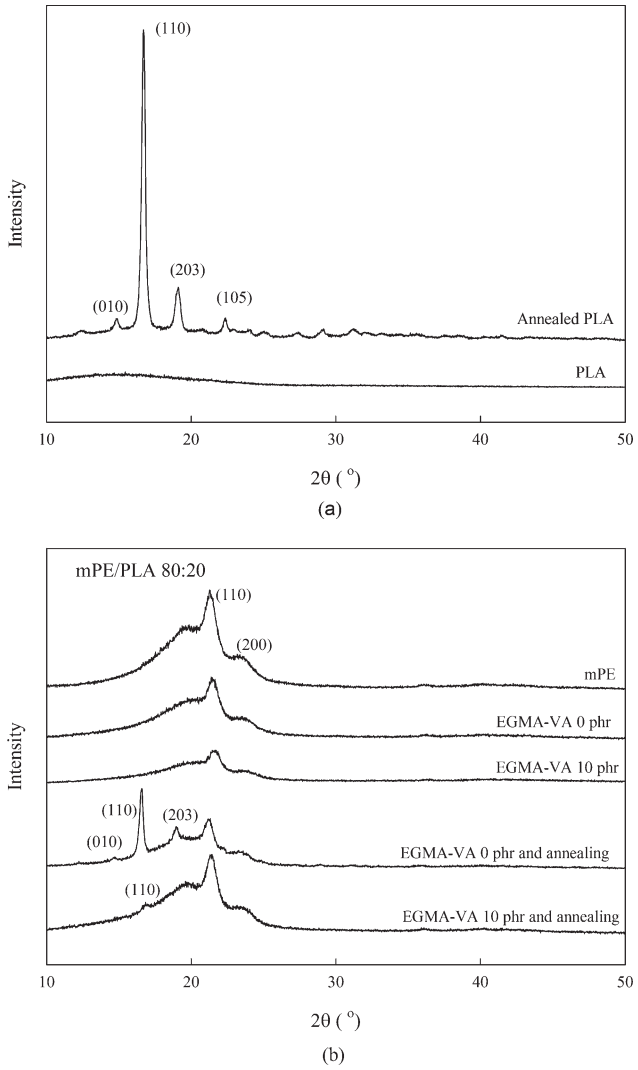

Figure 2. XRD patterns of (a) neat PLA and annealed PLA, (b) mPE/PLA blends.

traces did not vary much as listed in Table I. Yet, for the annealed PLA, additional tiny peak regarding the rearrangement crystallization at 156.2°C was also observed, accompanying a slight shift of cold crystallization. This type of crystallization behavior was also reported by Oyama[18] on the cold crystallization and rearrangement crystallization of PLA at 100.4 and 155.2°C, respectively. However, the annealing effect in the molding machine should be eliminated after the melting process in the DSC scan. It is unexpectedly to see this small difference for PLA with or without annealing after a second run. It seemed that annealed PLA "memorized" the highly ordered state even in the melt condition, and there is a need to pursue this interesting phenomenon in the future.

To get an insight perspective on the annealing effect after the preparation of the blends, Figure 6(a) delineates the first heating process of mPE/PLA blends at 10°C/min. Only slight variation on the melting behaviors of mPE was observed in the blends. As discussed in Figure 5(a) for neat PLA, the crystallinity of PLA in the blend without compatibilizer increased from

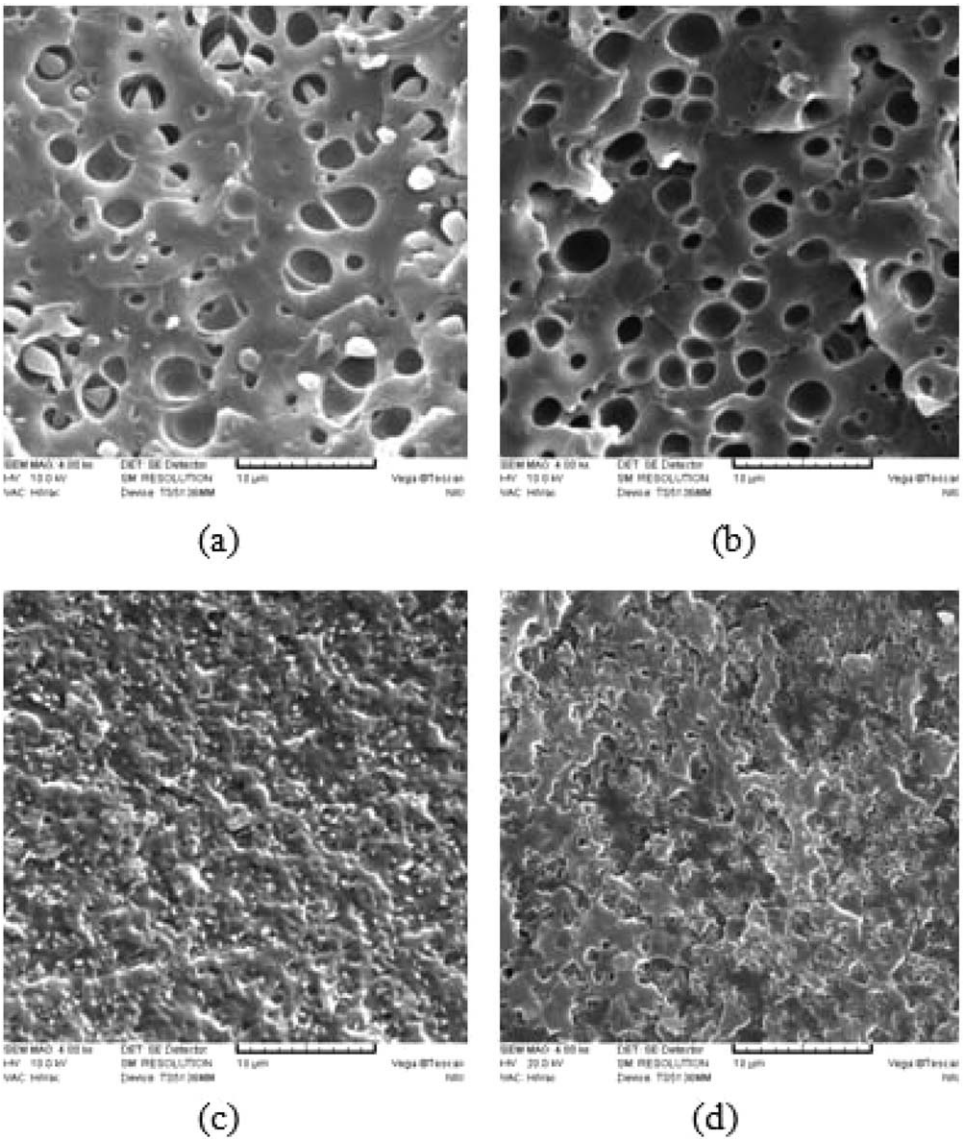

Figure 3. SEM micrographs of mPE/PLA blends with compatibilizer, (a) 0 phr, (b) 0 phr extracted by chloroform, (c) 10 phr, and (d) 10 phr extracted by chloroform.

9.7% (before annealing) to 32.7% (after annealing), although samples were not under controlled cooling process. It roughly justified the annealing effect on PLA in the compression molding machine. Further, the compatibilizer tended to suppress the crystallization rate of PLA, leading to the disappearance of cold crystallization and rearrangment crystallization of PLA due to the restriction of molecular chain mobility from its interaction with EGMA–VA, in agreement with XRD analysis. For the neat mPE/PLA blends after additional annealing treatment at 125°C for 2.5 h in the compression molding machine, the cold crystallization and rearrangement crystallization also were not visible, except the insignificant melting peak of PLA. Note that the annealing effect in the molding machine tended to assist imperfect crystals of PLA to be converted into more perfect crystals, as evidenced by the disappearance of cold crystallization peaks as seen in Figures 5(a) and 6(a). Likewise, for the compatibilized mPE/PLA blends with additional annealing treatment, the crystallization rate of PLA was suppressed, as seen in the compatibilized blends without the annealing treatment. Overall, the dominant effect from the compatibilizer on the crystallization of mPE/PLA blends in the later discussion of mechanical properties should be noted.

To further have a controlled thermal characterization at the same thermal history, the prepare blends were compared at a series of cooling and heating cycles, as shown in Figure 6(b) and (c). On cooling from the melt, the crystallization temperature of mPE was shifted from 61.2°C to 65.8°C with the addition of compatibilizer, and the crystallization temperature of EGMA–VA decreased slightly through its interaction with PLA. Basically, the thermal behaviors of blends with the annealing effect in this controlled cooling condition were essentially the same as

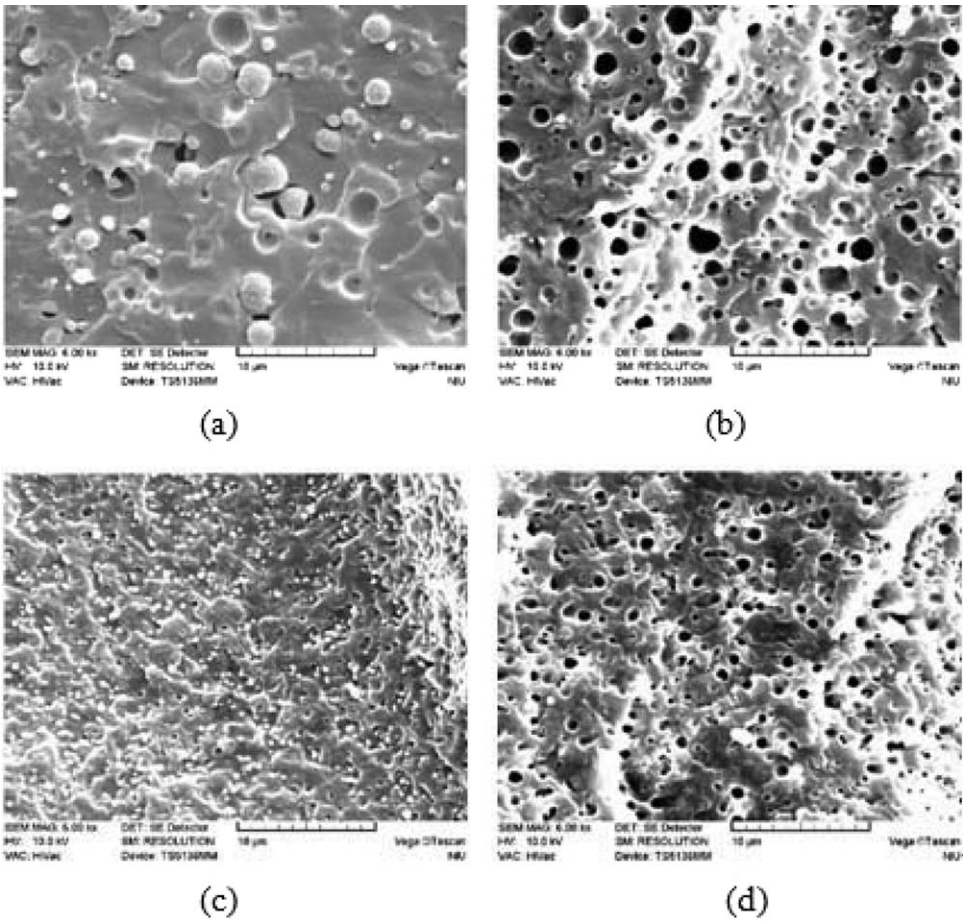

Figure 4. SEM micrographs of mPE/PLA blends with compatibilizer after annealing, (a) 0 phr, (b) 0 phr extracted by chloroform, (c) 10 phr, and (d) 10 phr extracted by chloroform.

those without annealing effect, as the annealing effect in the molding machine was eliminated after the melting process in the DSC scan.

Further discussion on the melting behaviors of samples in the second heating process at 10°C/min is investigated in Figure 6(c). The neat blends without the annealing treatment showed the similar behaviors as in the first heating process. Then, the crystallinity difference before and after annealing became marginal as seen in Table I for the second heating traces under the same controlled cooling in the DSC scan, since the thermal history was ruled out. With the addition of EGMA–VA in the mPE/PLA systems, the melting peaks of PLA were indiscernible, mainly attributed to the restriction of molecular chain mobility from its interaction with EGMA–VA, as mentioned earlier. In addition, the melting temperatures of mPE and PLA of mPE/PLA blends without compatibilizer remained largely unchanged as those of neat resins. Again, the thermal behaviors of blends with the annealing effect in this controlled heating condition were essentially the same as those without the annealing effect, as the annealing effect in the molding machine was eliminated after the melting process in the DSC scan.

Dynamic Mechanical Behaviors

Storage modulus of mPE/PLA blends is depicted in Figure 7(a). For brevity and comparison, the results for neat resins are depicted in Table II. The storage modulus of mPE/PLA blends generally increased with the addition of the compatibilizer mainly due to the enhanced interaction through the effectiveness of the EGMA–VA. The neat blends with the annealing treatment did not outperform the compatibilized blends without the annealing treatment, indicating the dominant role of improved compatibility over the annealing process. In addition, the highest storage modulus was attained for compatibilized mPE/PLA blends subjected to the annealing effect, suggesting the synergistic roles of both compatibilization and annealing effects. Apparently, annealing effect was also beneficial to the enhanced rigidity as annealed PLA gave the highest stiffness as seen in Table II.

Figure 7(b) shows tan δ as the function of temperature for mPE/PLA blends with or without compatibilizer/annealing effects. For comparison, Table II also shows the glass transition temperatures of neat resins based on the peak tan δ maximum (curves are omitted for brevity). As some tan δ peak transition curves were kind of broad and not easy to be precisely

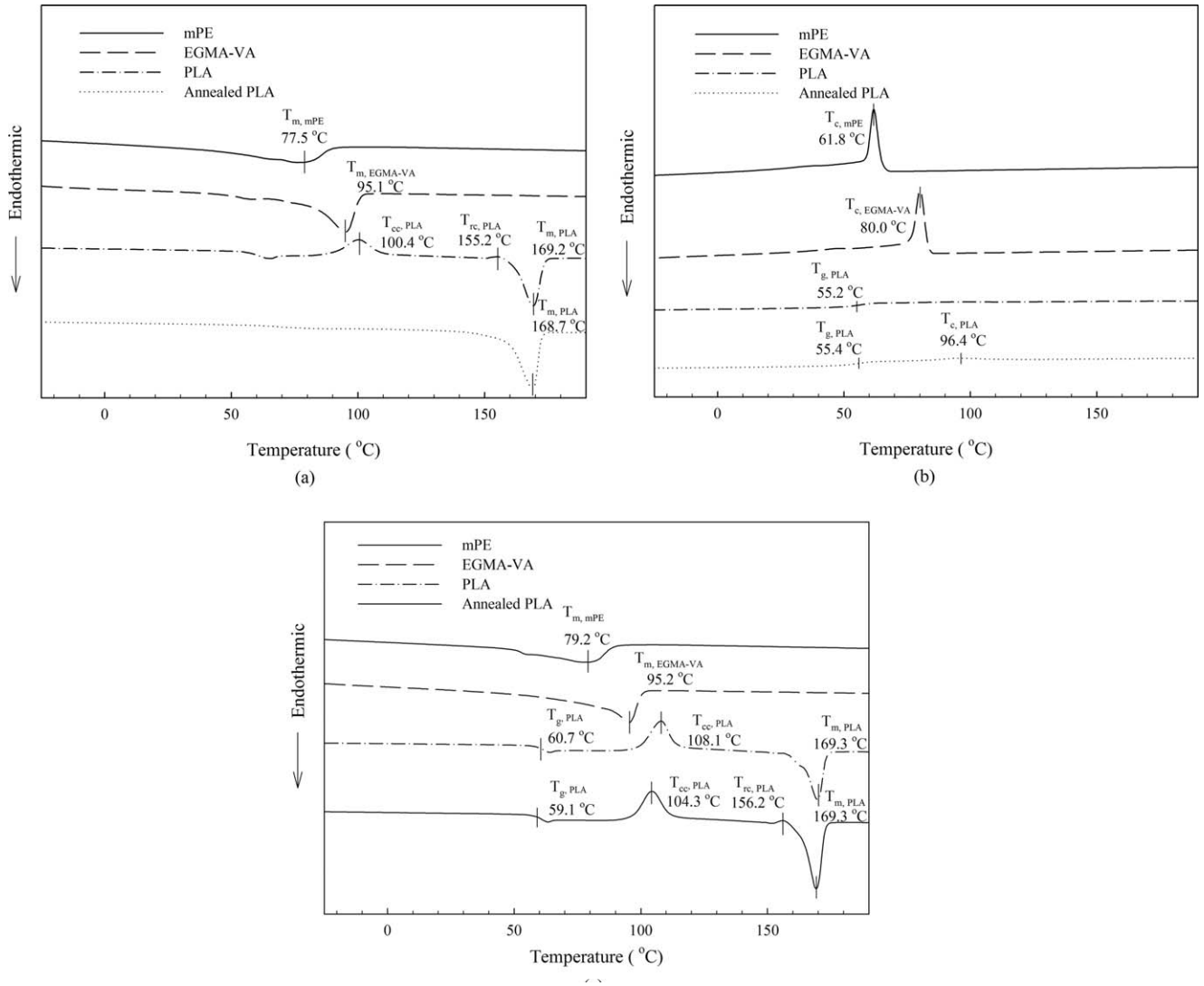

Figure 5. DSC thermograms of neat resins under 10°C/min rate (a) first heating, (b) cooling, (c) second heating.

identified as the peak maximum, so only the representative data were displayed. A slightly higher glass transition temperature (66.1°C) of annealed PLA than that of PLA without annealing was observed due to the restriction of molecular mobility due to the crystallization effect. Previous DSC traces in Figure 5(a) did not clearly reveal the glass transition temperature of annealed PLA in the first heating scan due to the similar reason. The broad peak values for the compatibilized mPE/PLA blends without annealing treatment tended to decrease due to the reduced dissipation through the higher interfacial interaction between mPE and PLA. Through this compatibilization effect, T_g values of PLA within the blends shifted slightly from 68.2°C to 64.9°C through the enhanced interaction between mPE and PLA. A similar situation was found for annealed samples with the help of the compatibilizer.

Mechanical Properties

The effects of compatibilizer loading and annealing treatment on tensile strength and Young's modulus of mPE/PLA blends are shown in Figure 8. Tensile strength increased with the addition of EGMA–VA for mPE/PLA blends without the annealing treatment, which was attributed to the enhanced interfacial interaction as evidenced in FTIR and SEM analyses. With the further annealing treatment on the compatibilized blends by exploiting the crystalline yielding effect from dispersed PLA domains through the annealing effect, as seen in XRD analysis, the tensile strength increased further up to 38% in comparison with the blends without the compatibilizer and annealing treatment. Thus, the synergistic effects by compatibilization and annealing treatment were of benefit in improving the tensile strength of the blends.

To further elucidate the tensile properties, Young's modulus of mPE/PLA blends is illustrated in Figure 8(b). Young's modulus of mPE/PLA blends without compatibilization and annealing treatment was about 30.6 ± 1.0 MPa. With the addition of compatibilizer, Young's modulus increased due to aforementioned enhanced interfacial interaction between mPE and PLA.

Table I. DSC Results of mPE/PLA Blends

	Process								
	Second heating						Cooling		
Sample code	T_{m1}[a] (°C)	T_{m2}[b] (°C)	T_{cc}[c] (°C)	T_{rc}[d] (°C)	T_g (°C)	X_c[e] (%)	T_{c1}[f] (°C)	T_{c2}[g] (°C)	T_g (°C)
mPE	79.2	-	-	-	-	-	61.8	-	-
PLA	-	169.3	108.1	-	60.7	8.9	-	-	55.2
PLA (annealed)	-	169.3	104.3	156.2	59.1	9.4	-	-	55.4
mPE/PLA/EGMA-VA (0 phr)	77.9	167.2	99.7	155.0	-	11.0	61.2	-	-
mPE/PLA/EGMA-VA (10 phr)	78.7	-	-	-	-	-	65.8	77.9	-
mPE/PLA/EGMA-VA (0 phr and annealing)	78.7	168.0	98.9	155.4	-	10.8	61.7	-	-
mPE/PLA/EGMA-VA (10 phr and annealing)	79.4	-	-	-	-	-	65.6	77.5	-

[a] T_m of mPE.

[b] T_m of PLA.

[c] Cold crystallization of PLA.

[d] Rearrangement crystallization of PLA.

[e] Crystallinity of PLA

[f] T_c of mPE.

[g] T_c of EGMA-VA.

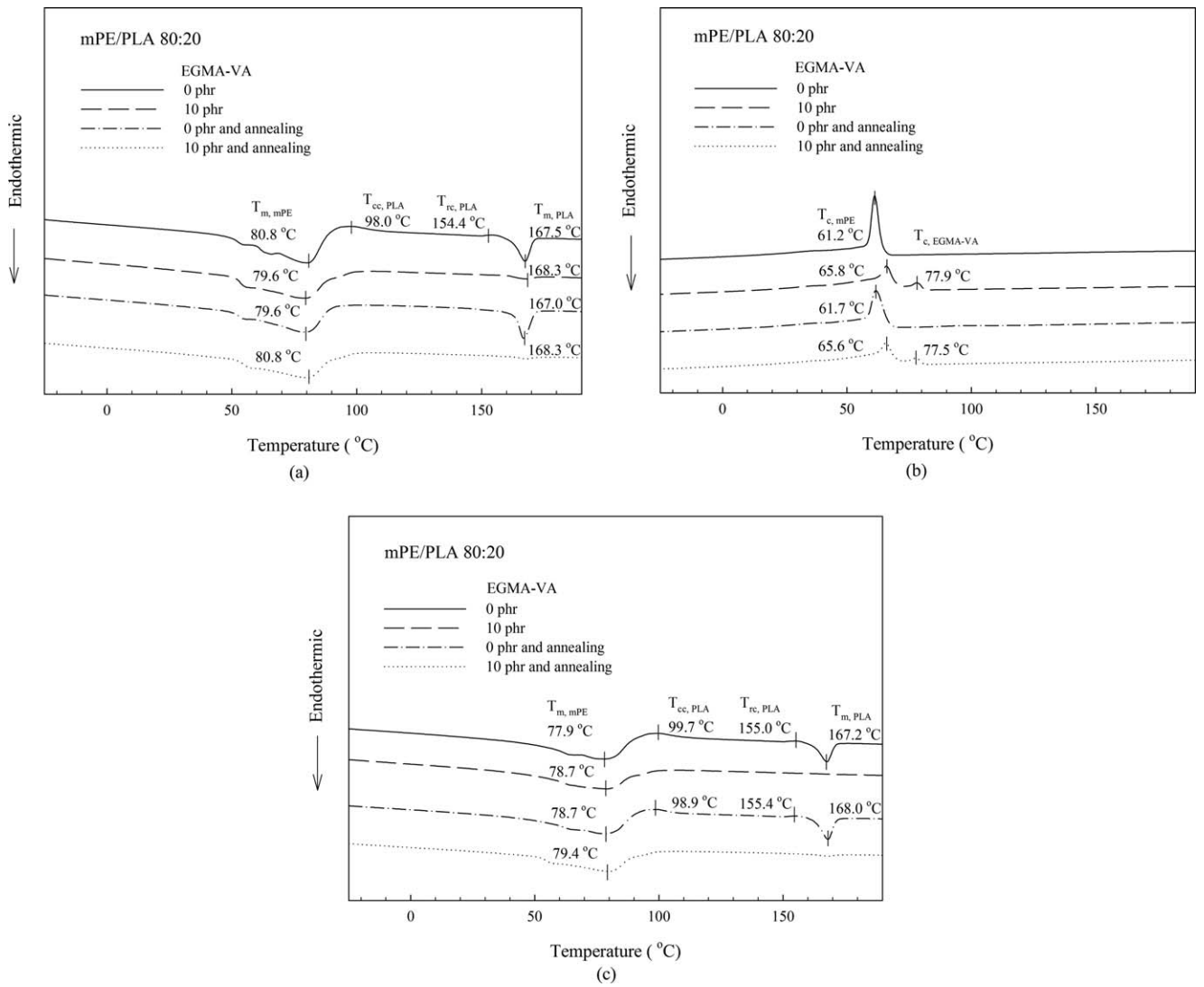

Figure 6. DSC thermograms of mPE/PLA blends under 10°C/min rate (a) first heating, (b) cooling, and (c) second heating.

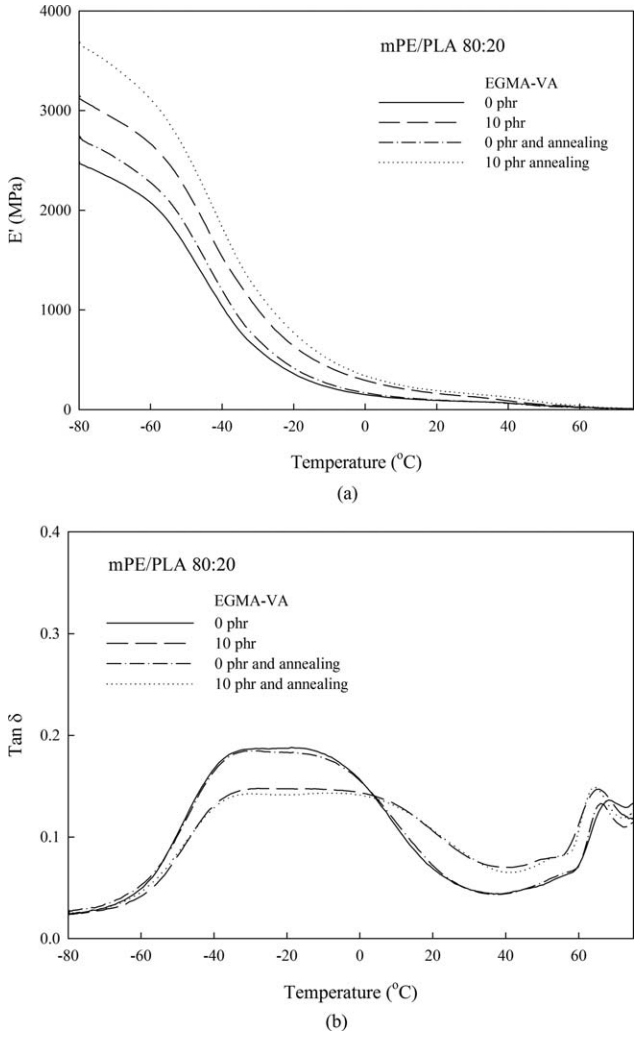

Figure 7. DMA of mPE/PLA blends (a) storage modulus (E') and (b) tan δ.

A further annealing treatment on the compatibilized blends led to the highest Young's modulus, 49.7 ± 2.1 MPa, among the investigated systems. Apparently, the additional rigidity contributed from re-crystallized PLA also played an important role in the stiffness enhancement of the prepared blends. In general, the improved interfacial interaction between the mPE matrix and PLA domains and the additional annealing effect did confer an observable difference in mechanical properties. However, as seen in DSC and XRD analyses, the compatibilizer also tended to suppress the crystallization rate of PLA, thus the dominant effect from the compatibilizer to improve the mPE and PLA interaction over the annealing effect to promote crystalline formation should be recognized in the consideration of tensile properties.

Figure 8(c) also shows the elongation at break of mPE/PLA blends. Elongation at break of mPE/PLA blends without compatibilization and annealing treatment was about 975.3 ± 18.3%. With the addition of compatibilizer, elongation at break decreased to 808.1 ± 56.4% due to aforementioned enhanced interfacial interaction between soft mPE and rigid PLA. A similar decrement was found for the annealed samples with the addition of compatibilizer. As mentioned in the discussion of Young's modulus, the compatibilizer tended to suppress the crystallization rate of PLA, thus the dominant effect on the elongation at break from the compatibilization over the annealing effect was also observed.

To further get some understanding on the tensile properties of neat resins, the results of mPE and PLA before and after annealing were listed in Table III. Basically, there was not much difference in the tensile properties of mPE after annealing, except a small decrement in the elongation at break. On the other hand, an increment, up to 35%, in the Young's modulus of PLA was observed, which was attributed to the increased crystallization behavior as seen in the DSC. This increment would contribute to the enhancement in the tensile strength and Young's modulus of the blends, even though the compatibilizer somehow suppressed the crystallization rate as discussed earlier.

In addition to tensile properties, a brief impact test was also conducted. However, unlike the conventional systems where the PLA matrix were filled with elastomeric polymer to improve their impact strength, all investigated systems in this study

Table II. DMA Results of mPE/PLA Blends

Sample code	EGMA-VA (phr)	Storage modulus at 25°C (MPa)	$T_{g,\ PLA}$ (°C)	T_g (°C)	$T_{g,mPE/EGMA-VA}$[a] (°C)
mPE	-	86.2	-	−30.0	
PLA	-	3354.4	62.2	-	
PLA (annealed)	-	6100.3	66.1	-	
EGMA-VA	-	235.2	-	−15.3	
mPE/PLA/EGMA-VA	0	86.4	68.2	-	−23.5
	10	143.3	64.9	-	−16.2
mPE/PLA/EGMA-VA annealing	0	87.6	67.0	-	−22.3
	10	171.4	64.2	-	−16.5

[a] A discernible transition between mPE and EGMA-VA.

Applied Polymer SCIENCE

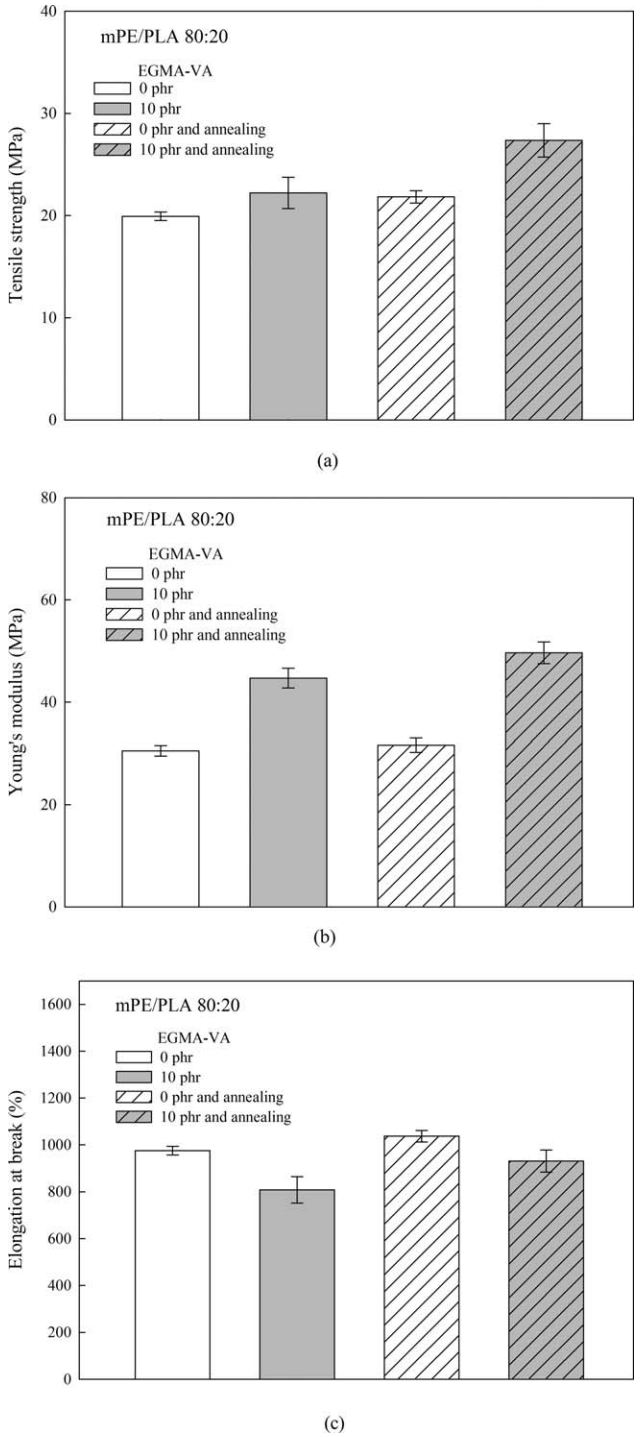

Figure 8. Tensile properties of mPE/PLA blends (a) tensile strength, (b) Young's modulus, and (c) elongation at break.

showed non-break phenomena due to the elastomeric property of mPE matrix, except that the impact strength of neat PLA resin slightly increased from 20.8 ± 0.3 J/m (before annealing) to 22.8 ± 0.3 J/m (after annealing). This unexpected small increase was mainly attributed to the increased entangled density of molecular chains for annealed PLA observed in the literature.[18]

Table III. Tensile Properties of mPE and PLA

Sample code	Properties		
	Tensile strength (MPa)	Young's modulus (MPa)	Elongation at break (%)
Before annealing			
mPE	25.3 ± 1.3	23.8 ± 1.7	1043.0 ± 29.3
PLA	47.1 ± 2.4	1700.8 ± 134.9	4.9 ± 0.3
After annealing			
mPE	26.1 ± 2.1	23.4 ± 0.9	920.4 ± 21.8
PLA	37.2 ± 4.6	2298.4 ± 139.0	3.3 ± 0.5

Rheological Properties

To further elucidate the interfacial interaction of mPE and PLA through the rheological analysis, the shear viscosity for mPE/PLA blends with or without compatibilizer is shown in Figure 9. The viscosity of mPE/PLA blends followed the general trend of rheological behaviors for polymeric materials and decreased with increasing shear rate, except for neat PLA due to its polyester nature with Newtonian behavior. For viscosity at high shear rates, the measured values became scattered due to the limitation of equipment. The viscosity of mPE was more than 10-fold higher than that of PLA. Owing to the significant difference in the viscosity ratio and chemical affinity, mPE and PLA blends tended to give an incompatible blend. As a result, the viscosity of blends incorporating only 20% of PLA was slightly lower than that of mPE. With the incorporation of compatibilizer, EGMA–VA, the viscosity increased and reached the highest level among all neat resins and blends, which was attributed to the enhanced interfacial interaction through the possible formation of EGMA–VA–PLA copolymer. Note that this viscosity increment of compatibilized blends was not from the viscosity contribution of EGMA–VA compatibilizer, as its value was still lower than that of neat mPE. Overall, rheological properties could be a useful tool to evaluate the interaction degree of mPE and PLA through the help of compatibilizer.

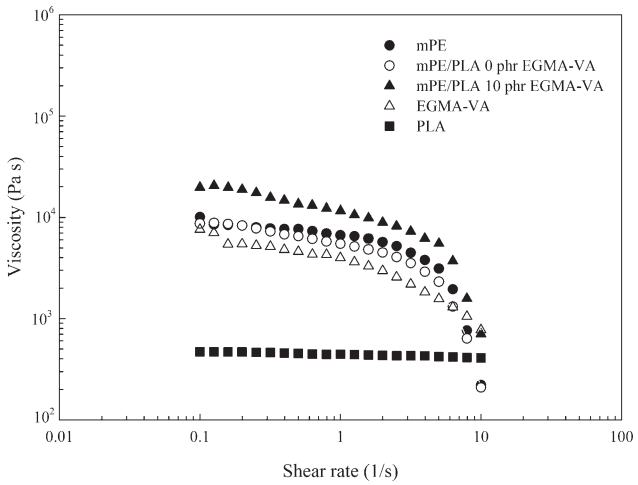

Figure 9. Viscosity (Pa s) versus shear rate (1/s) curves of mPE/PLA blends.

CONCLUSIONS

The properties of metallocene polyethylene (mPE)/PLA bio-based blends containing an ethylene–glycidyl methacrylate–vinyl acetate (EGMA–VA) compatibilizer, with or without annealing effect of PLA were investigated. The results from SEM morphology observation, FTIR analysis, and rheological study revealed that the interaction between the mPE matrix and dispersed PLA enhanced with the addition of the compatibilizer. DSC and XRD results indicated that the addition of the compatibilizer completely hindered the cold crystallization and rearrangement crystallization of PLA, even though the additional annealing effect of mPE/PLA blends in the molding machine tended to increase the crystallization of PLA. Tensile test results showed that the synergistic effects by compatibilization and annealing treatment improved the tensile strength and Young's modulus, up to 38 and 62% increase, respectively. Hopefully, the incorporated bio-based PLA materials could be helpful in reducing the use of petroleum-based materials and are beneficial to the environment in terms of the sustainable development concern.

ACKNOWLEDGMENTS

A grant-in-aid from the R.O.C government under NSC 98-2622-E-197-002-CC3 is greatly acknowledged. The authors are grateful to Mr. C.-W. Huang for helping manuscript preparation.

REFERENCES

1. Kweon, D.-K.; Cha, D.-S.; Park, H.-J.; Lim, S.-T. *J. Appl. Polym. Sci.* **2000**, *78*, 986.
2. Ray, S. S.; Okamoto, M. *Macromol. Rapid Commun.* **2003**, *24*, 815.
3. Singh, G.; Bhunia, H.; Rajor, A.; Jana, R. N.; Choudhary, V. *J. Appl. Polym. Sci.* **2010**, *118*, 496.
4. Anderson, K. S.; Lim, S. H.; Hillmyer, M. A. *J. Appl. Polym. Sci.* **2003**, *89*, 3757.
5. Pai, F.-C.; Chu, H.-H.; Lai, S.-M. *J. Polym. Eng.* **2011**, *31*, 463.
6. Su, Z.; Li, Q.; Liu, Y.; Hu, G.-H.; Wu, C. *Eur. Polym. J.* **2009**, *45*, 2428.
7. Magoń, A.; Pyda, M. *Polymer* **2009**, *50*, 3967.
8. Gupta, A. P.; Saroop, U. K.; Gupta, V. *J. Appl. Polym. Sci.* **2007**, *106*, 917.
9. Lopez-Rubio, A.; Flanagan, B. M.; Gilbert, E. P.; Gidley, M. J. *Biopolymers* **2008**, *89*, 761.
10. You, Y.; Youk, J. H.; Lee, S. W.; Min, B.-M.; Lee, S. J.; Park W. H. *Mater. Lett.* **2006**, *60*, 757.
11. Chandra, R.; Rustgi, R. *Polym. Degrad. Stab.* **1997**, *56*, 185
12. Miyata, T.; Masuko, T. *Polymer,* **1998**, *39*, 5515.
13. Wang, H.; Zhang, Y.; Tian, M.; Zhai, L.; Wei, Z.; Shi, T. *J. Appl. Polym. Sci.* **2008**, *110*, 3985.
14. Kister, G.; Cassanas, G.; Vert, M. *Polymer* **1998**, *39*, 267.
15. Tsai, C.-H.; Chang, F.-C. *J. Appl. Polym. Sci.* **1996**, *61*, 321.
16. Das, K.; Ray, D.; Banerjee, I.; Bandyopadhyay, N.R.; Sengupta, S.; Mohanty, A.; Misra, M. *J. Appl. Polym. Sci.* **2010**, *118*, 143.
17. Chiu, F.-C.; Lai, S.-M.; Ti, K.-T. *Polym. Test.* **2009**, *28*, 243.
18. Oyama, H. T. *Polymer* **2009**, *50*, 747.